ELSEVIER

Thermochimica Acta 271 (1996) 93–100

thermochimica
acta

Calorimetric investigations in a dispersion strengthened 7075 alloy[1]

W. Lacom

Austrian Research Centre Seibersdorf, A-2444 Seibersdorf, Austria

Received 22 May 1995; accepted 12 June 1995

Abstract

Isothermal microcalorimetry and DSC thermal analysis were carried out on mechanically alloyed 7075 (AlZnMgCu), containing 1 vol% of Al_2O_3-dispersoids , or 1 vol% Al_2O_3- plus 4 vol% Al_4C_3-dispersoids in as-quenched, air-cooled and artificially aged conditions in order to study the decomposition behaviour, and its implications for strengthening mechanisms. From combined DSC and isothermal calorimetry, it is inferred that the low hardening potential of P/M dispersion strengthened 7075 is due to irreversible loss of solute atoms rather than because of excess vacancy reduction. It is concluded that magnesium atoms undergo spinell reactions with Al_2O_3-dispersoids during high temperature processing (i.e. reaction annealing for Al_4C_3 formation), thereby reducing the potential for precipitation hardening.

Keywords: Calorimetry; Aluminium alloys; Precipitation; Dispersoids

1. Introduction

In order to extend high strength levels in aluminium alloys to temperatures above 200°C, ceramic particulates in the size range of 10–20 μm are introduced into age hardening alloys of the 2xxx, 6xxx and 7xxx type [1]. However, the particulates' strength contribution, thought to stem from high dislocation densities, that are created during cooling, due to the high mismatch of thermal expansion between matrix and particulates is rather low. In the case of strengthening by high volume fractions of Al_4C_3-dispersoids in the size range of some 10 nm, the Orowan mechanism is operative, resulting in values

---

[1] Presented at the 11th Ulm Conference, Freiberg, 29–31 March, 1995.

SSDI 0040-6031 (95) 02579-0

for the yield strength of ca. 360 MPa [2]. In order to further increase strength levels, it seems attractive to introduce Al_4C_3-dispersoids into a matrix of the AlZnMgCu system, which offers strength values of 500 MPa due to η'-precipitation. However, hardness measured in such a material produced by mechanical alloying and reaction annealing showed only little response to age hardening [3]. It is the purpose of this contribution to substantiate these findings and to provide explanations for the underlying mechanism.

2. Experimental conditions

Wrought 7075-type material PRS, with 6% Zn, 2.5% Mg and 1.5% Cu was obtained from AMAG in the homogenized and extruded condition. It then was shred to flakes of about 1 mm, milled for 2 h in an attritor, cold-compacted and extruded at 450°C to obtain alloy OC. By this procedure a 1% volume fraction of Al_2O_3-dispersoids in the size range of 10–30 nm is introduced as a result of oxygen pick-up during milling.

Alloy 2C was produced by incorporation of 2 wt% of graphite flakes into the PRS matrix by attritor milling and formation of ca. 4 vol% Al_4C_3-dispersoids with diameters from 30 to 80 nm upon subsequent reaction annealing (3–5 h, 550°C).

Isothermal ageing at 130°C was followed in a heat flow microcalorimeter of the Tian-Calvet type on cylindrical samples ($9.5\phi \times 67\ mm^3$) that were contained in metallic and graphitic sample holders. Due to thermal perturbations during sample introduction, the beginning of the heat evolution cannot be detected before 40 min; it then was observed for about 24 h. For further experimental details see Ref. [3].

Thermal analysis was performed within a Perkin Elmer DSC II at a heating rate of $40\ K\ min^{-1}$ between room temperature and 845 K on disc-like samples ($6\phi \times 1\ mm^3$), lying in BN-pans. The baselines were taken from measurements on pure aluminium; the peak enthalpies were determined with the aid of a data-processing unit. Due to the baseline uncertainty, the enthalpy values are affected by a mean uncertainty of ca. $1\ J\ g^{-1}$.

Solutionizing for 30 min at 470°C was done in air, while rapid quenching was carried out in cold water and slow cooling in air; 130°C ageing was either performed in the microcalorimeter or in an oil-bath. Measurements were repeated for each condition at least twice; reproducibility was ca. 1% for thermal analysis and ca. 5% for microcalorimetry.

3. Experimental results

3.1. DSC: as quenched condition (AQ)

Thermoanalytical curves of the AQ condition given in Fig. 1 show the rather complex decomposition behaviour for the pure matrix alloy (PRS). Between room temperature (RT) and about 500 K two overlapping exothermal effects with a total enthalpy content of $-7.6\ J\ g^{-1}$ are detected. The region from 500 to 600 K is characterized by superposition of several endo- and exothermal effects; it is followed by a wide endothermal reaction with ca. $26.0\ J\ g^{-1}$, and at about 750 K the thermal baseline is attained.

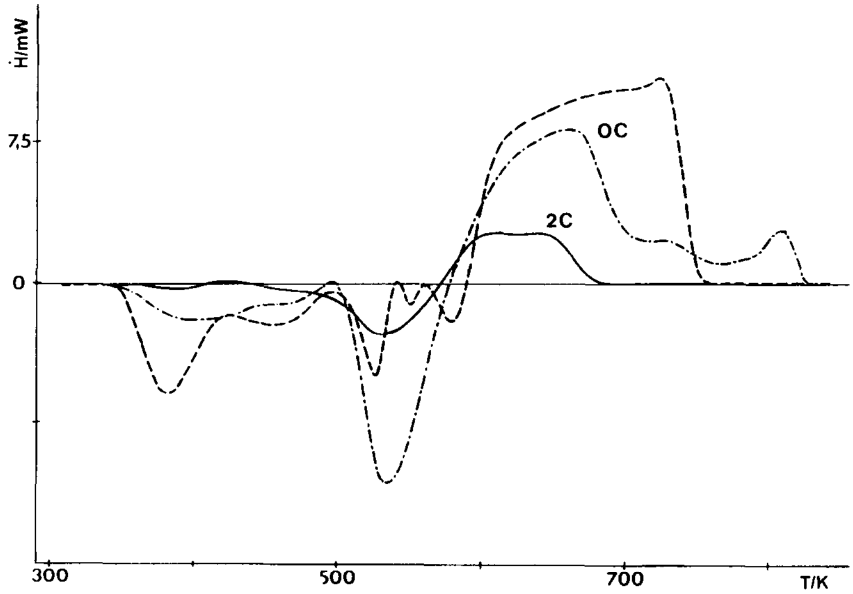

Fig. 1. Thermoanalytical curves of pure matrix alloy and for alloys OC and 2C in the as-quenched condition measured at a heating rate of 40 K $\min^{-1}$.

With alloy OC the two exothermals between RT and 500 K and the high temperature endothermal (ca. –3.1 and 14.3 J g^{-1}) are significantly diminished; the complicated structure between 500 and 600 K is replaced by a single exothermal effect with an enthalpy content of –9.3 J g^{-1}. In the case of 2C the low temperature exothermal effects are hardly detectable; the following exothermal has been reduced to –3.1 J g^{-1}, the endothermal to 4.7 J g^{-1}.

3.2. Air-cooled condition (AC)

Owing to slow cooling, in Fig. 2 for all three alloys, the low temperature exothermal effects have disappeared, as well as the complicated structure for PRS between 500 and 600 K which is replaced by a simple exothermal. The exothermal effects of OC and 2C are much smaller than in the AQ condition; this is not the case for the endothermal effects. A comparison of the major thermal effects (in J g^{-1}) for conditions AQ and AC is given in Table 1.

3.3. Artificial ageing (5 h, 130°C; 24 h, 130°C) after water quenching

Thermoanalytical curves given in Fig. 3 for 5 h ageing exhibit endothermal maxima at about 480 K, with enthalpy contents of ca. 8.0 and 4.3 J g^{-1} for PRS and OC, respectively, and 1.0 J g^{-1} for 2C. The endothermals in the high temperature range are similar to those observed in AQ and AC conditions. Between 500 and 600 K the measured curve

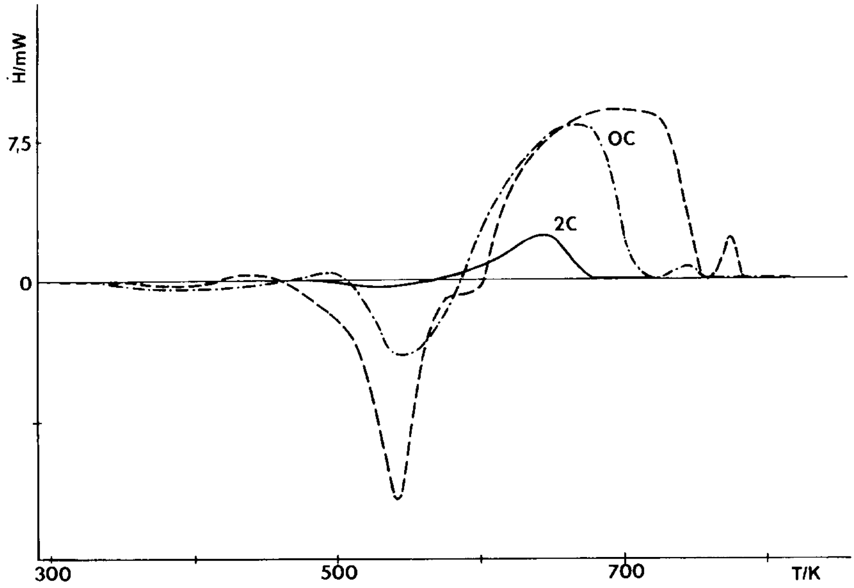

Fig. 2. Thermoanalytical curves of pure matrix alloy and for alloys OC and 2C in the air-cooled condition measured at a heating rate of 40 K min^{-1}.

for PRS and also for OC is best described by a superposition of a large exothermal and a smaller endothermal effect; alloy 2C exhibits only a small exothermal reaction.

Upon prolonged ageing at 130°C the 480 K endothermals are considerably increased, as well as the endothermal of PRS and OC around 540 K; for OC even the endothermal region is attained; alloy 2C does not exhibit any exothermal effect at all. The enthalpy values (in J g^{-1}) for 5 and 24 h at 130°C are given in Table 2.

3.4. Isothermal microcalorimetry

Fig. 4 gives account of the heat release rate $-\dot{H}$ of alloys OC and 2C upon ageing at 130°C after water quenching from 475°C.

Table 1
Enthalpy content of peaks (in J g^{-1})

	Thermal effect (*T*–range)					
	Exothermal (RT–500 K)		Exothermal (500–600 K)		Endothermal (600–750 K)	
	AQ	AC	AQ	AC	AQ	AC
PRS	−7.6	~0	−5.4	~0	26.0	21.4
OC	−3.1	~0	−9.3	−4.0	14.3	12.9
2C	~0	~0	−3.1	−0.2	4.7	2.6

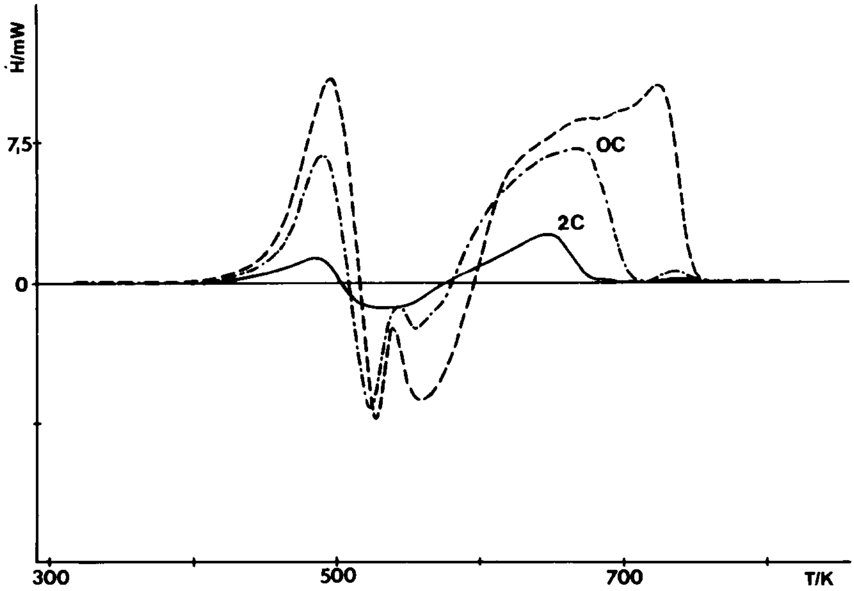

Fig. 3. Thermoanalytical curves of pure matrix alloy and for alloys OC and 2C after water quenching and 5 h, 130°C ageing at a heating rate of 40 K min^{-1}.

The curves exhibit a slow decay of $-\dot{H}$ with its maximum situated before 40 min and thus not detectable. Alloy OC shows a very strong exothermal effect which is somewhat reduced in comparison to that found in the monolithic PRS matrix. In the case of 2C, however, a reduction by almost one order of magnitude reflects a drastic change between the two alloys.

4. Discussion

In order to interpret the reduced decomposition rate of alloys OC and 2C it is useful to refer first to the monolithic alloy PRS.

Table 2

Enthalpy content of peaks

	Ageing	
	5 h, 130°C	24 h, 130°C
PRS	8.0	10.1
OC	4.3	6.9
2C	1.0	3.5

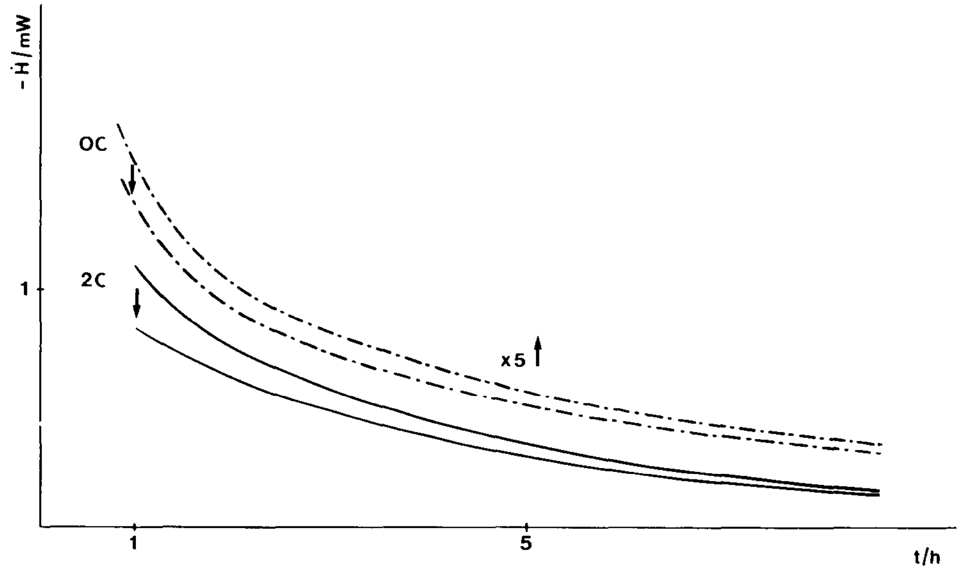

Fig. 4. Heat release rate of alloys OC and 2C at 130°C ageing after water quenching.

4.1. Alloy PRS

Several TEM and/or DSC investigations have been performed on this type of alloy [5,6]; however, an unambiguous identification of the various thermal effects is not at hand. Based on previous work on AlZnMg alloys [7,8] for the as-quenched condition, the first exothermal effect in Fig. 1 is associated with formation of GP zones which, around 450 K, are transformed to metastable phase precipitates of the η'-type. The complicated structure between 500 and 600 K is supposed to be due to massive formation of the η equilibrium phase (exothermal effect) which is superimposed by simultaneous dissolution of η'-precipitates (endothermal effect). η' formed during quenching and η' formed via GP zones would give rise to a double dissolution peak. Above 600 K the wide endothermal of about 26 J g^{-1} reflects dissolution of equilibrium precipitates formed during quenching as well as during the DSC run. Summing up all endo- and exothermal effects, a value Σ of about 13 ± 1 J g^{-1} signals an important volume fraction of precipitates (η' and some η) already present after water quenching.

In the case of slow cooling, Fig. 2 shows that, due to massive η-precipitation before the DSC scan, supersaturation is too low for formation of GP zones and η'-precipitates in the DSC, and only between 500 and 600 K is additional η-formation possible. This results in a simple exothermal reaction, which is not superimposed by η'-dissolution as in the AQ condition. The sum of all exo- and endothermal effects $\Sigma \approx 11 \pm 1$ J g^{-1} shows that the degree of precipitation during water quenching and slow cooling is similar; however, the type of precipitates (η respectively η') is quite different.

Ageing at 130°C after water-quenching results in the massive formation of fine metastable precipitates, which are associated with GP zones of enhanced size and stability;

their volume fraction shows an increase when ageing time is increased from 5 to 24 h. In both cases, GP zone dissolution is followed by η-precipitation superimposed by some η'-dissolution and, finally, η-dissolution as in the AQ condition.

4.2. Alloys OC and 2C

In comparison to PRS in the water quenched condition, GP zone formation during the DSC run is greatly diminished in OC and practically non-existent in 2C. No η'-dissolution is observed in either alloy, and precipitation of the η-phase in the DSC between 500 and 600 K accounts for about 75% of the total η-volume fraction dissolved at higher temperatures. In both cases, $\Sigma \leq 2 \pm 1$ J g^{-1} indicates that only very little precipitation occurs during the quenching procedure; the small dissolution effect at 800 K in OC reflects the presence of some very stable, heterogeneously formed η-precipitates. Comparing the three alloys, it becomes obvious that in OC and 2C the decomposition processes of the PRS matrix are significantly affected and diminished.

The same tendency prevails after slow cooling (Fig. 2), with the fraction of η-precipitates present before the DSC measurement being higher in OC and 2C because heterogeneous nucleation of η-particles on dispersoids is favoured by the slow cooling rate.

The results of the water-quenched and air-cooled samples reveal that

- due to the addition of dispersoids, the kinetics and/or the driving force for precipitation of excess Zn and Mg atoms is drastically reduced;
- dispersoids, therefore, can effectively act as heterogeneous nuclei only at a slow cooling rate.

In principle, reduced precipitation effects can be the result of a diminished excess vacancy concentration; in the case of OC and 2C the dispersoids and dislocations introduced during cooling are thereby likely to slow down diffusion.

However, the results of isothermal ageing at 130°C cannot be interpreted just on the basis of reduced diffusion rates for OC and 2C, as no shift of the maximum of the isothermal $\dot{H}$-curves is indicated, and even after 24 h the η'-volume fraction remains low for OC and 2C. Furthermore, as can be seen from all DSC measurements, even in the higher temperature range, where quenched-in excess vacancies are less important, precipitation effects are low in alloys containing dispersoids.

Therefore, after ruling out kinetic effects, it can only be concluded that a decreased amount of solute atoms is responsible for the observed diminution of precipitation in OC and 2C. The only possibility for solute atoms to be lost irreversibly is thought to be related to the Al_2O_3-dispersoids, which have been shown to undergo reactions with Mg atoms at high temperatures according to

$$Al_2O_3 + 3Mg = 3MgO + 2Al \quad \text{or} \quad Al_2O_3 + Mg = Mg_2AlO_4 \tag{1}$$

Spinell formation has been observed in 6061/Al_2O_3 after high temperature exposure [9] using STEM methods. In alloy OC these reactions would be likely to occur upon extrusion at 450°C and solutionizing at 470°C, whereas in alloy 2C much more magnesium is lost during the prolonged reaction annealing process at 550°C.

5. Conclusions

The calorimetric investigations confirm the low hardening potential of dispersion strengthened 7075 alloy produced by a P/M process, as found by hardness measurements.

From combined DSC and isothermal microcalorimetry measurements, it is concluded that the age-hardening response of the 7075-matrix is diminished due to irreversible solute losses to Al_2O_3-dispersoids introduced during reactor milling.

As these losses cannot be avoided during extrusion and/or reaction annealing, in order to make use of precipitation hardening, a higher magnesium content would have to be envisaged.

References

[1] J.P. Hirth, Scripta Metal., 25 (1991) 1.

[2] G. Jangg, in E. Arzt, and L. Schultz (Eds.), New Materials by Mechanical Alloying Techniques, DGM, Oberursel, 1988, p. 39.

[3] J. Zbiral, private communication

[4] A. Zahra, C.Y. Zahra, M. Laffitte, W. Lacom and H.P. Degischer, Z. Metallkd., 70 (1978) 172.

[5] J.K. Park, Mater. Sci. Eng. A, 103 (1988) 223.

[6] K. Asano and K. Hirano, Trans. Jpn. Inst. Met., 9 (1968) 24.

[7] H.P. Degischer, W. Lacom, A. Zahra and C.Y. Zahra, Z. Metallkd., 71 (1980) 231.

[8] A. Zahra, C.Y. Zahra, W. Lacom and H.P. Degischer, Mater. Sci., 17 (1982) 3068.

[9] Th. Schmitt, H. Kaufmann, H. Leitner, H.P. Degischer, W. Lacom and K. Spiradek, OEFZS-A-2443, December, 1993.